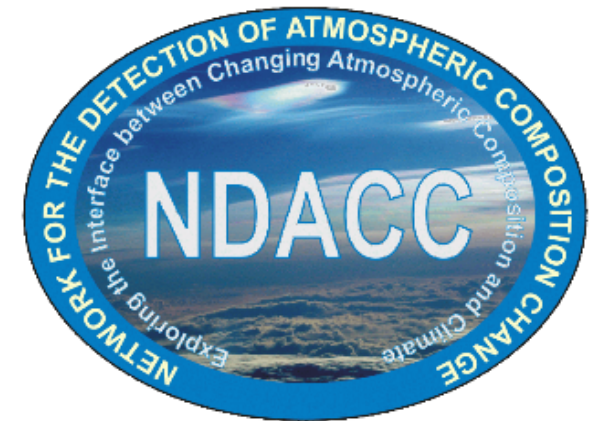


# Tropopause folds in North America studied from partial columns of trace gases measured at two ground-based sites

Ruben Pavia-Hernandez<sup>1</sup>, Michel Grutter<sup>1</sup>, Wolfgang Stremme<sup>1</sup>, Kimberly Strong<sup>2</sup>, and Shoma Yamanouchi<sup>2</sup>

<sup>1</sup>Centro de Ciencias de la Atmósfera, Universidad Nacional Autónoma de México, Mexico.

<sup>2</sup>Department of Physics, University of Toronto, Toronto, Canada.

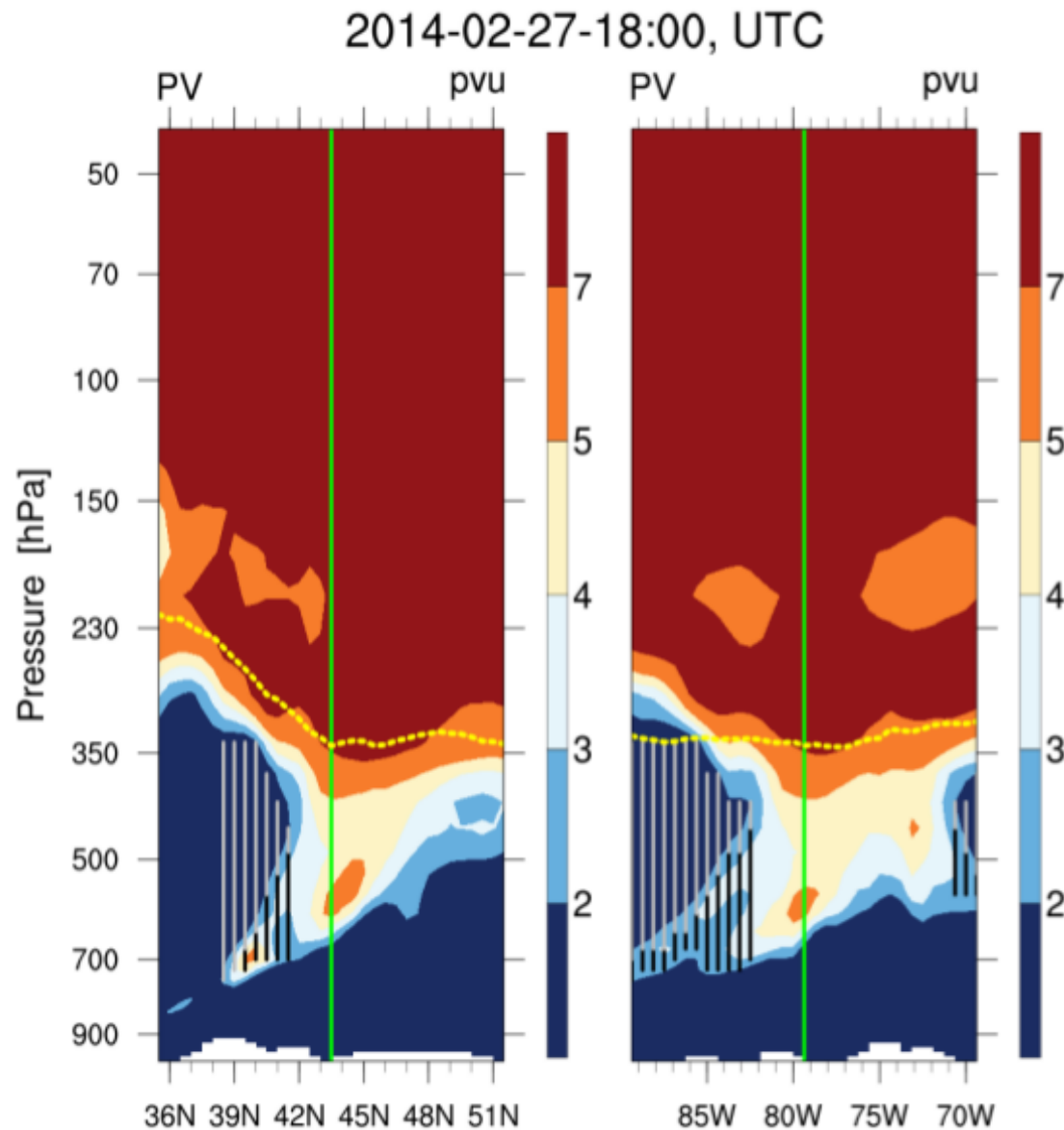


# **Why tropopause folds?**

They may be the dominant and most efficient stratosphere-troposphere exchange mechanism in mid-latitudes (Mohanakumar, 2008).

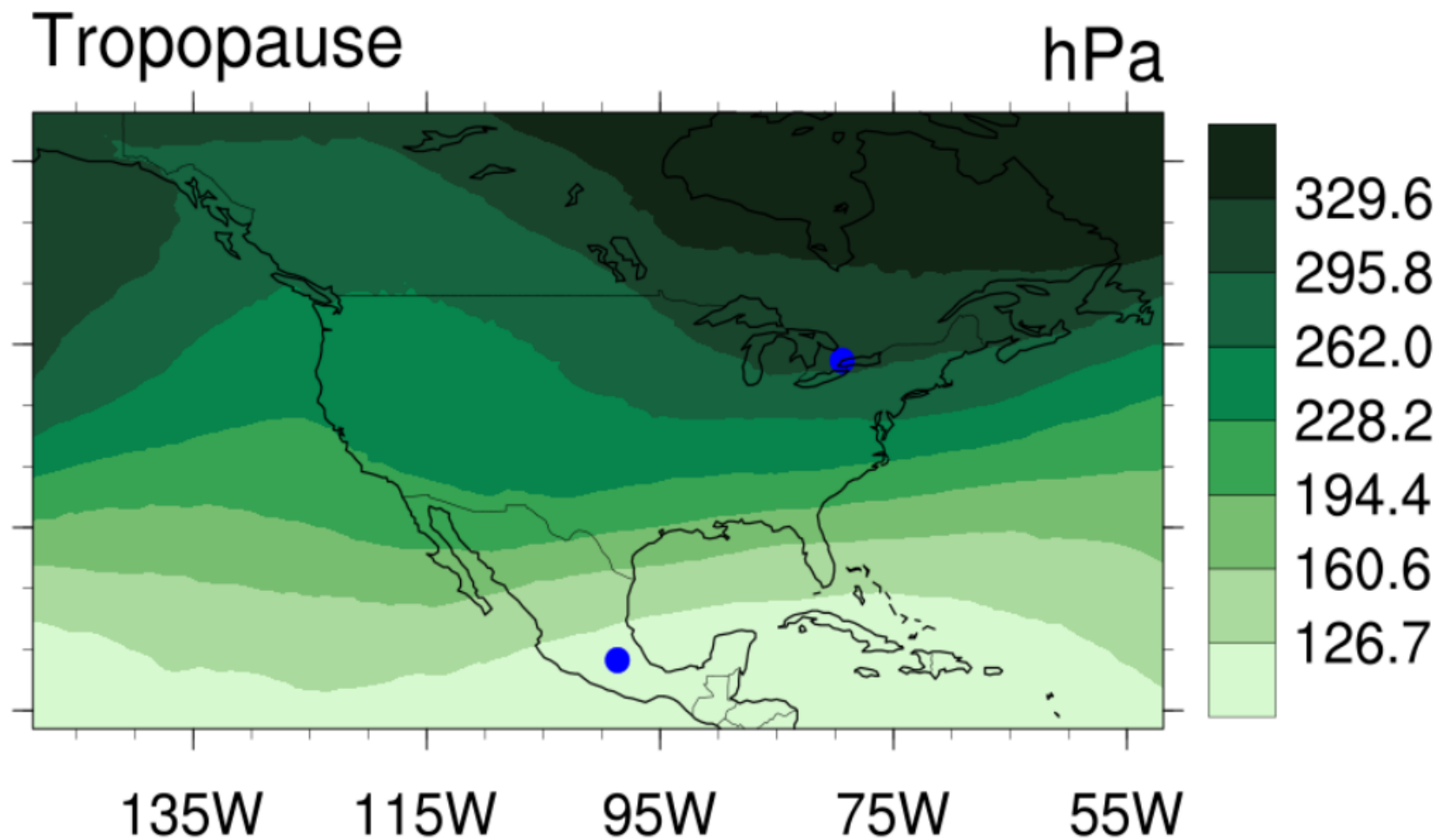
Folds can lead to ground-level ozone exceeding air quality standards in both subtropical and mid-latitudes (Barrett et al., 2019; Knowland et al., 2017).

The algorithm developed by Sprenger et al. (2003) was used in order to define whether there is a tropopause fold at a given location, by means of the potential vorticity (PV) and specific humidity ( $q$ ) fields from MERRA-2 reanalysis.



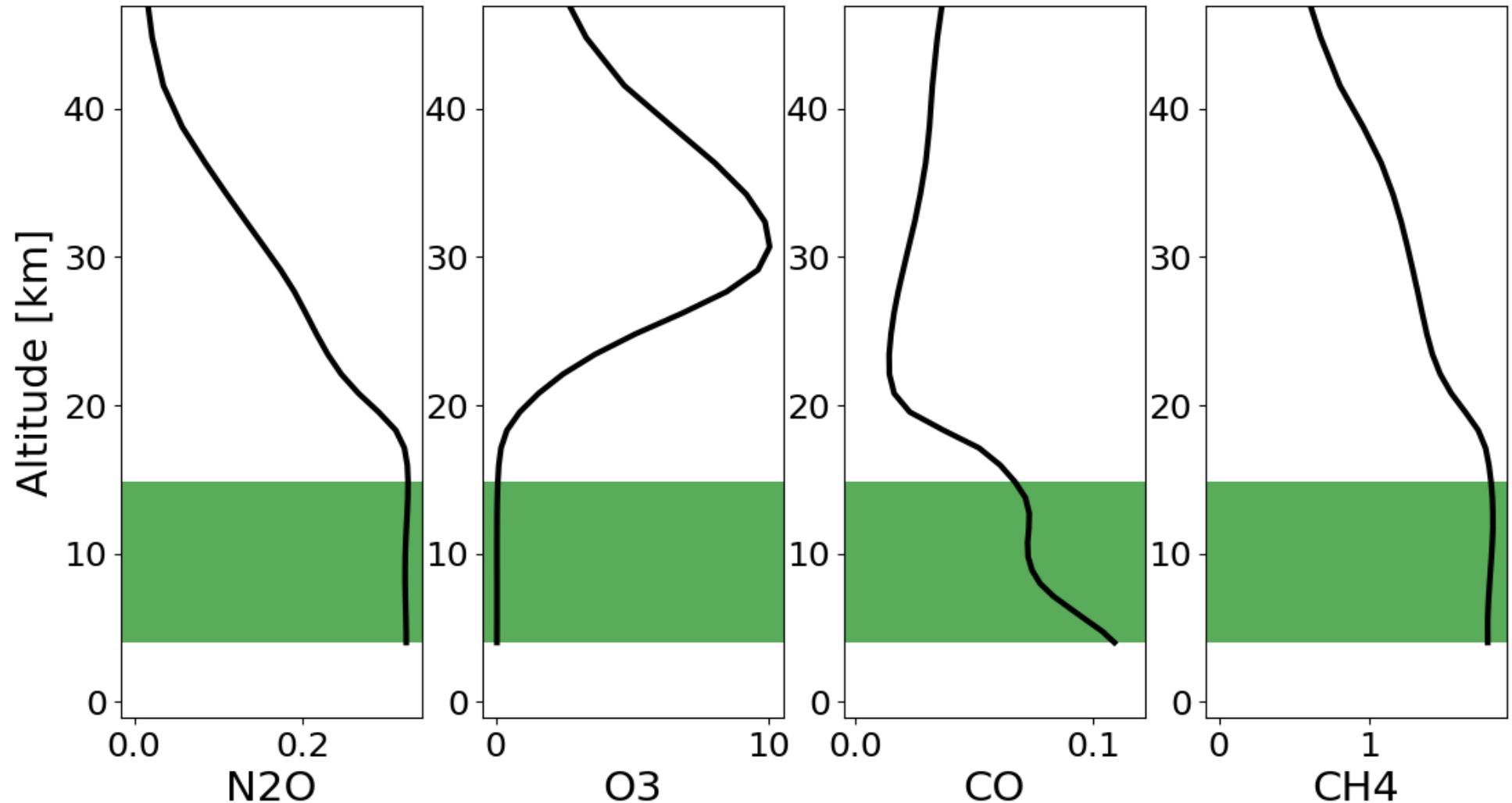
Air parcels were classified as **stratospheric** if  $PV > 2$  potential vorticity units (pvu) and  $q < 10^{-4} \text{ g kg}^{-1}$ .

Left: Cross-sections of the PV field centered at 43.5N, 79.37W (green vertical lines). At grid points where a fold is detected, gray and black vertical lines indicate the **gap** and **thickness** (both in hPa), respectively; the lowest level of the event (maximum pressure) constitutes its **depth**. Yellow dotted lines show the monthly average tropopause.

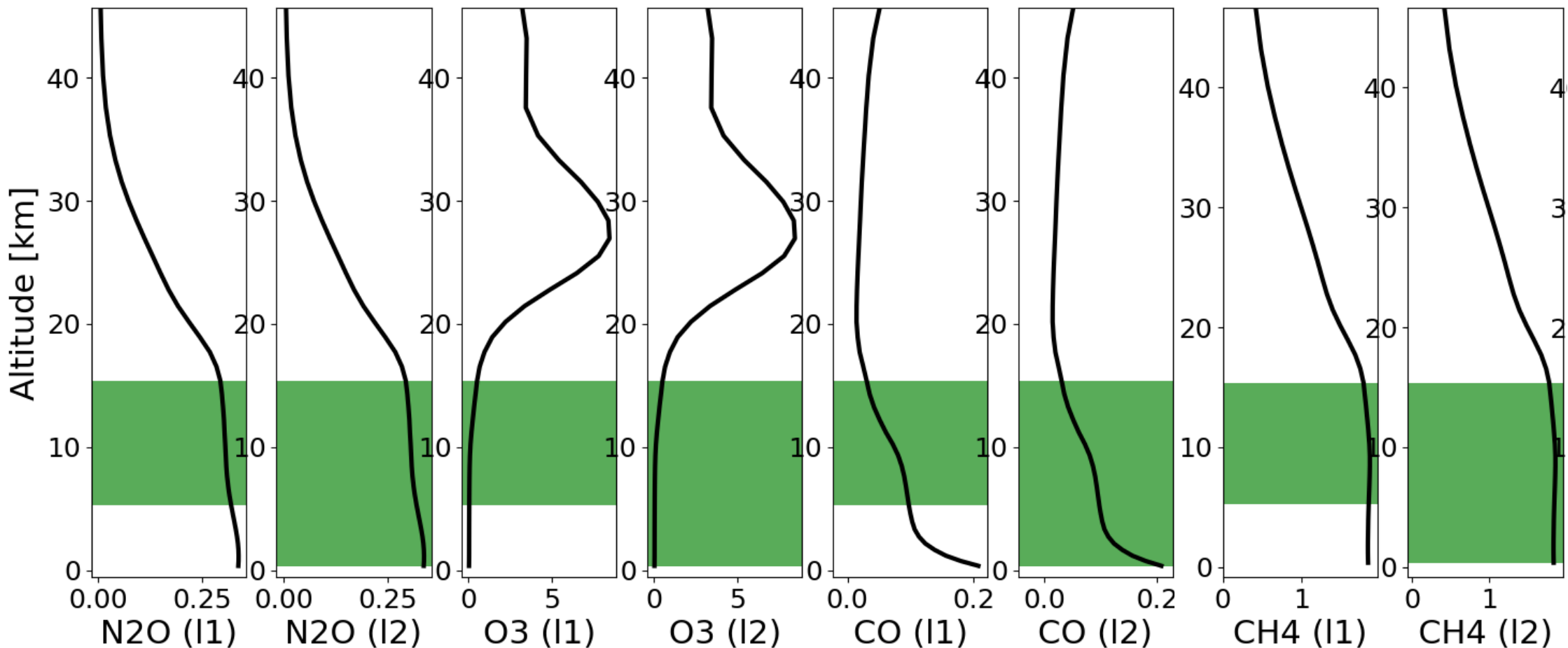


MERRA-2 domain for which PV and q fields were downloaded. Tropopause pressure, calculated from the 2 pvu threshold, is also shown. The two ground-based sites (**Altzomoni**, in central Mexico, and **Toronto**, in southern Canada), are indicated by the blue points. They contribute to the Infrared Working Group (IRWG), which is part of the Network for the Detection of Atmospheric Composition Change (NDACC).

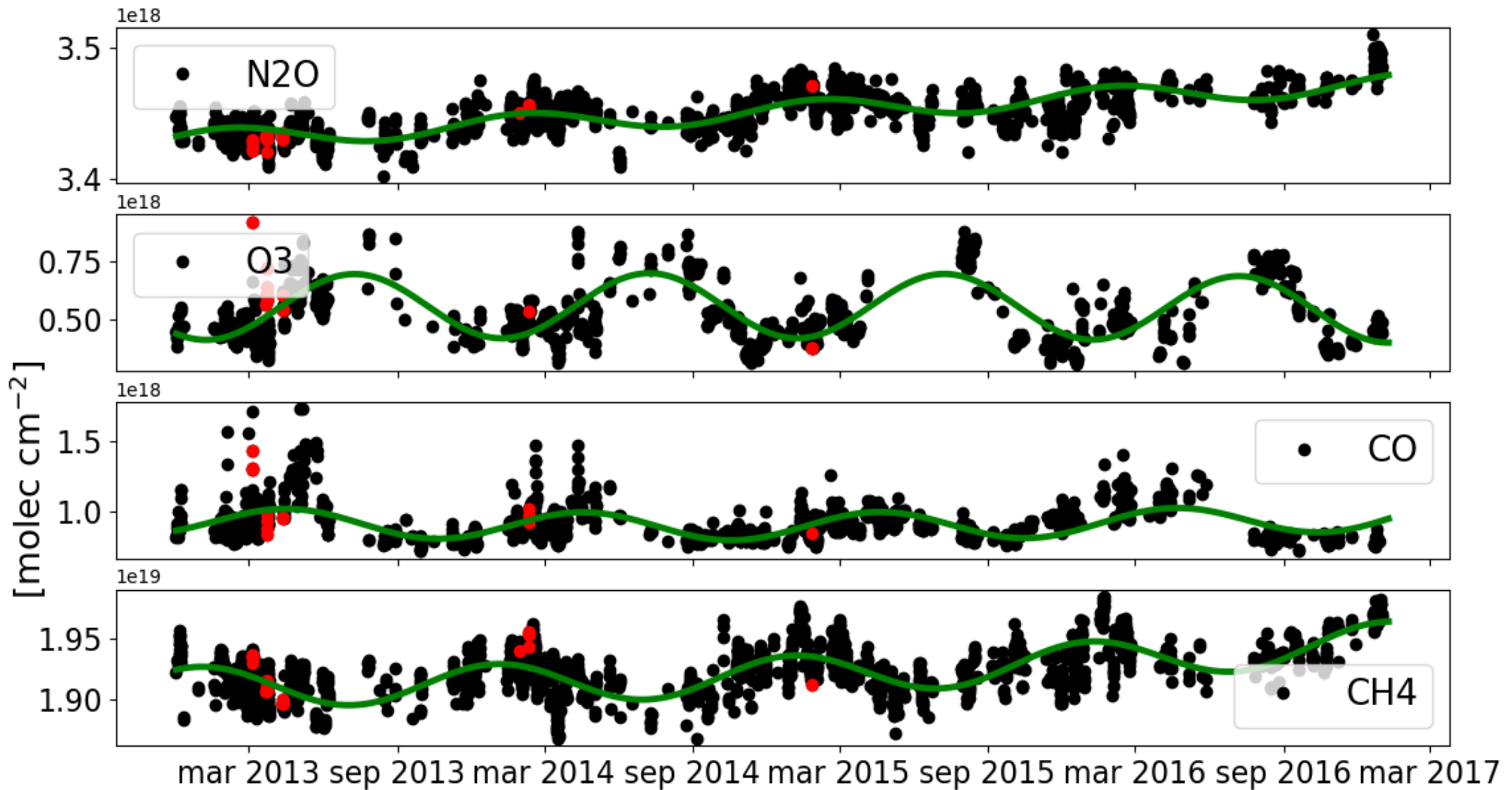
When infrared Fourier-transform spectra were measured during fold events, tropospheric partial columns (shaded levels in figure below) were retrieved for N<sub>2</sub>O, O<sub>3</sub>, CO and CH<sub>4</sub>.



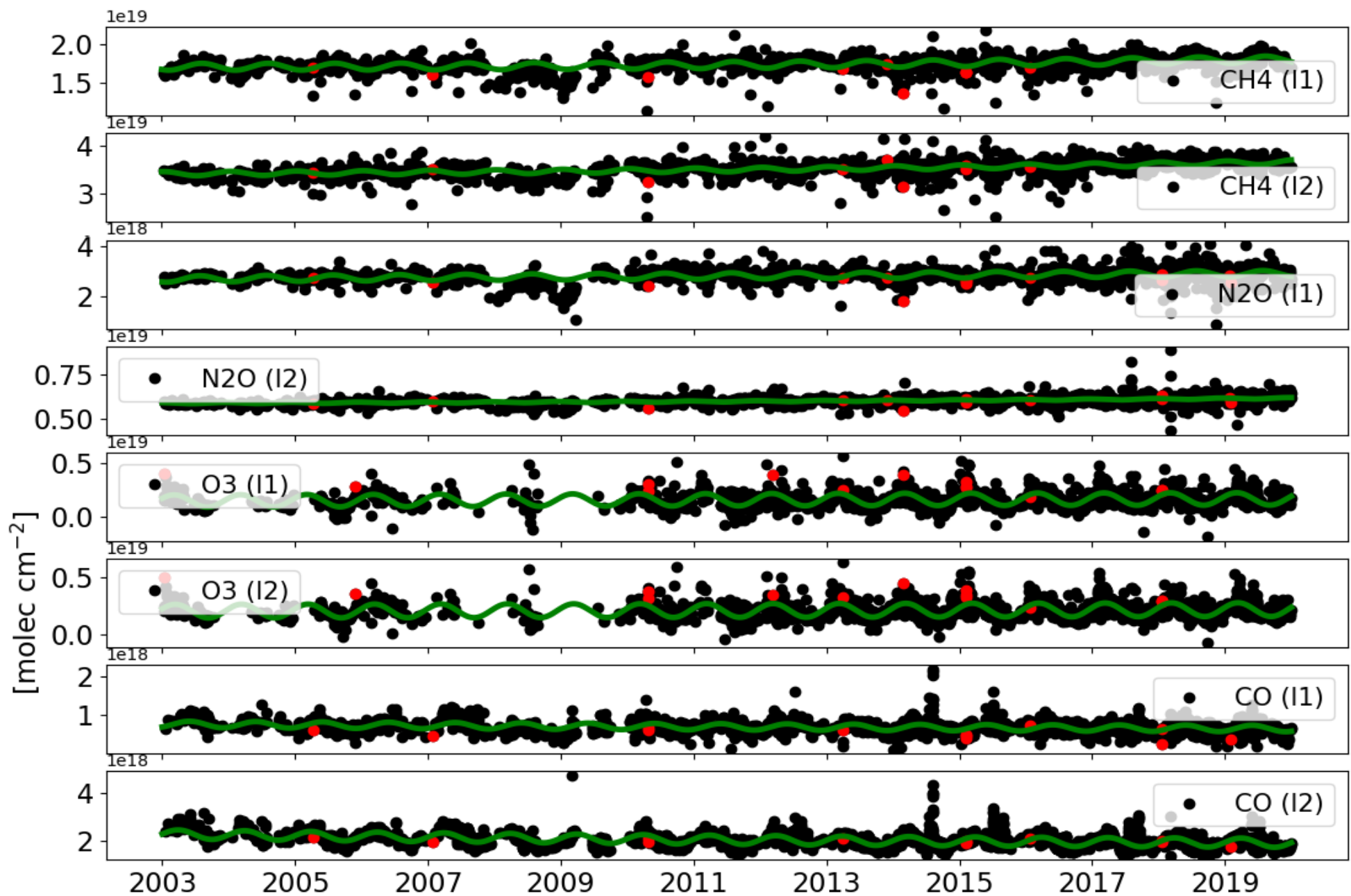
Average profiles of the gases, in ppmv, retrieved for **Altzomoni**. The shaded levels were chosen because retrievals accumulated at least 1 degree of freedom (mean and median of all retrievals).



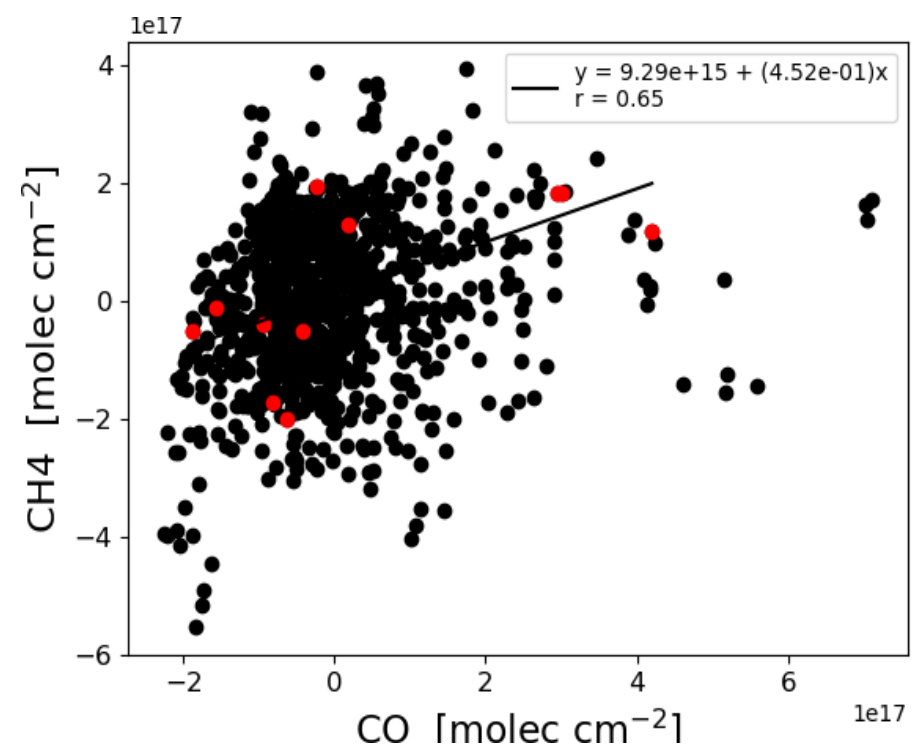
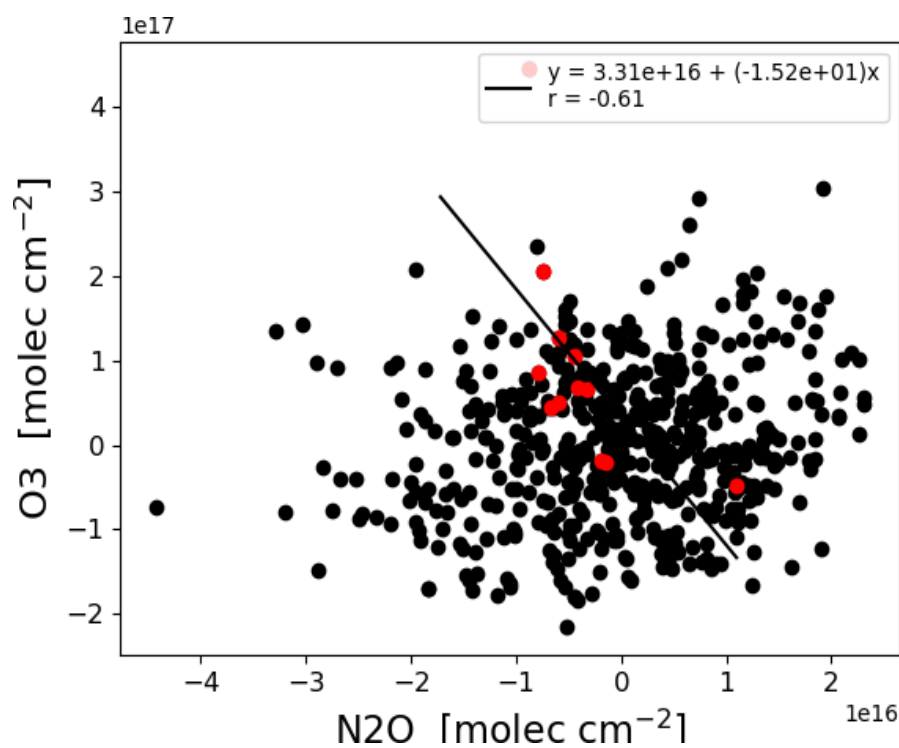
Average profiles of the gases, as in the previous figure, but for **Toronto**. Different levels were chosen because of the differences in accumulation of degrees of freedom: regions labeled as 'layer 1' **(I1)** and 'layer 2' **(I2)** correspond to partial columns between 5-15 km and 0.2-15 km, respectively.



Time series of the selected partial columns (1-hour averages) for **Altzomoni**. Green solid lines represent functions fitted to the data (constant, linear, parabolic and sinusoidal terms). Red dots show partial columns retrieved for hours when folds with thickness  $> 100$  hPa were detected.



Time series of the selected partial columns, as in the previous figure, but for **Toronto**. Red dots show partial columns retrieved for hours when folds with depth - pressure<sub>monthly avg</sub> (tropopause) > 380 hPa were detected.

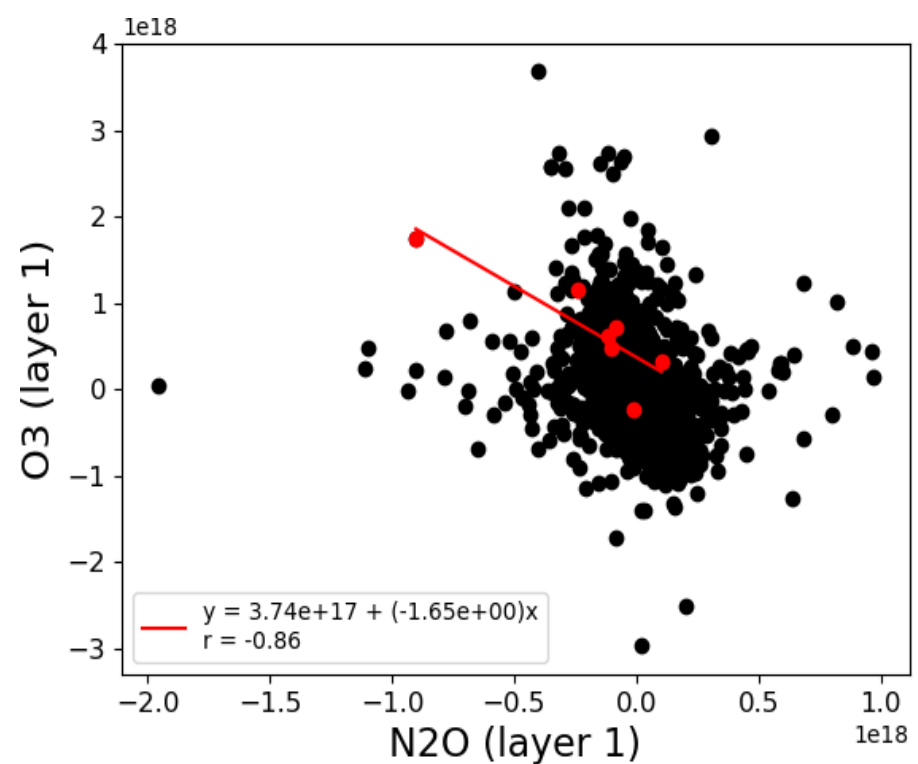
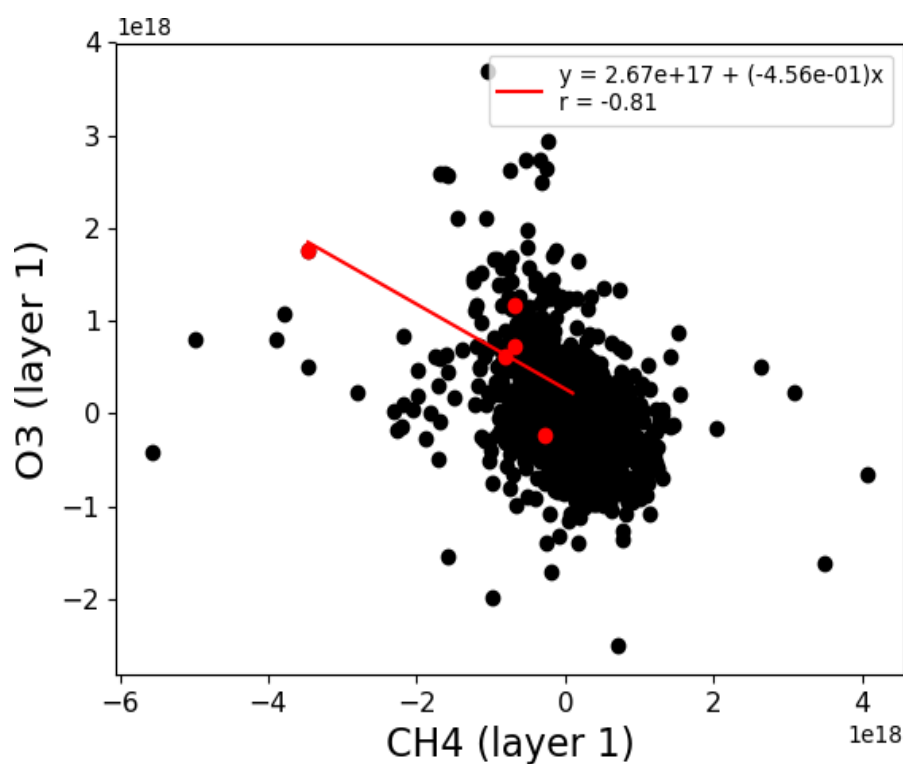


Scatter plots of partial columns retrieved for **Altzomoni**. Each partial column is plotted after subtracting the corresponding value of the fitted seasonal curve (green solid lines shown in the time series). Absolute values of correlation coefficients are greater when only partial columns selected during tropopause folds (red dots) are taken into account:

$$r_{\text{red dots}} (\text{N}_2\text{O}, \text{O}_3) = -0.61 \qquad r_{\text{all dots}} (\text{N}_2\text{O}, \text{O}_3) = 0.14$$

$$r_{\text{red dots}} (\text{CO}, \text{CH}_4) = 0.65 \qquad r_{\text{all dots}} (\text{CO}, \text{CH}_4) = 0.21$$

\*Vertical gradients of these species have the **same sign** for the pair CO-CH<sub>4</sub>, and **different signs** for the pair N<sub>2</sub>O-O<sub>3</sub> (see the vertical profiles).

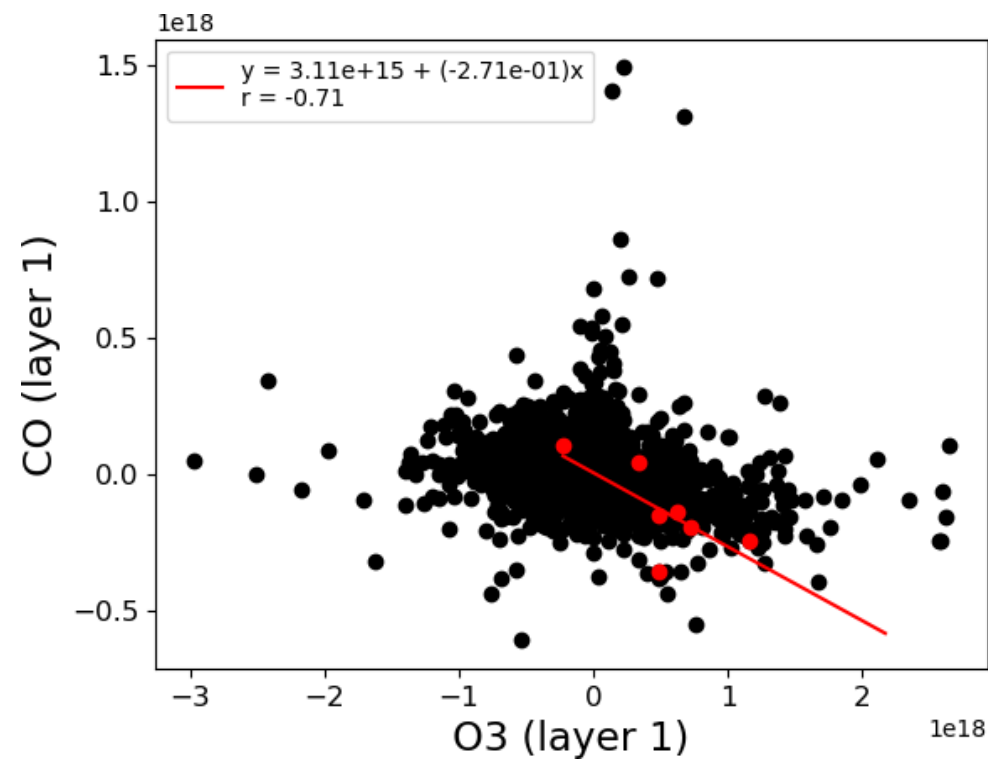


Scatter plots of partial columns, as in the previous figure, but for **Toronto**. Absolute values of correlation coefficients are greater when only partial columns selected during tropopause folds (red dots) are taken into account:

$$r_{\text{red dots}} (\text{CH}_4, \text{O}_3) = -0.81 \quad r_{\text{all dots}} (\text{CH}_4, \text{O}_3) = -0.36$$

$$r_{\text{red dots}} (\text{N}_2\text{O}, \text{O}_3) = -0.86 \quad r_{\text{all dots}} (\text{N}_2\text{O}, \text{O}_3) = -0.26$$

\*Vertical gradients of these species have **different signs** for the pairs  $\text{CH}_4\text{-O}_3$  and  $\text{N}_2\text{O-O}_3$  (see the vertical profiles).



$$r_{\text{red dots}} (\text{O}_3, \text{CO}) = -0.71$$

$$r_{\text{all dots}} (\text{O}_3, \text{CO}) = -0.27$$

\*Vertical gradients of these species have **different signs** for the pair  $\text{O}_3$ -CO (see the vertical profiles).

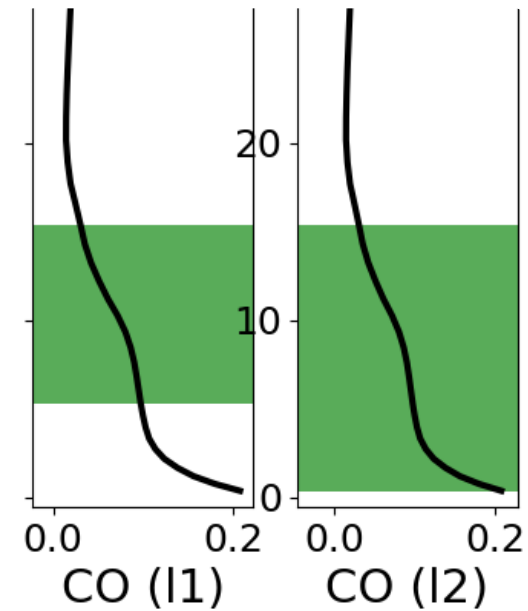
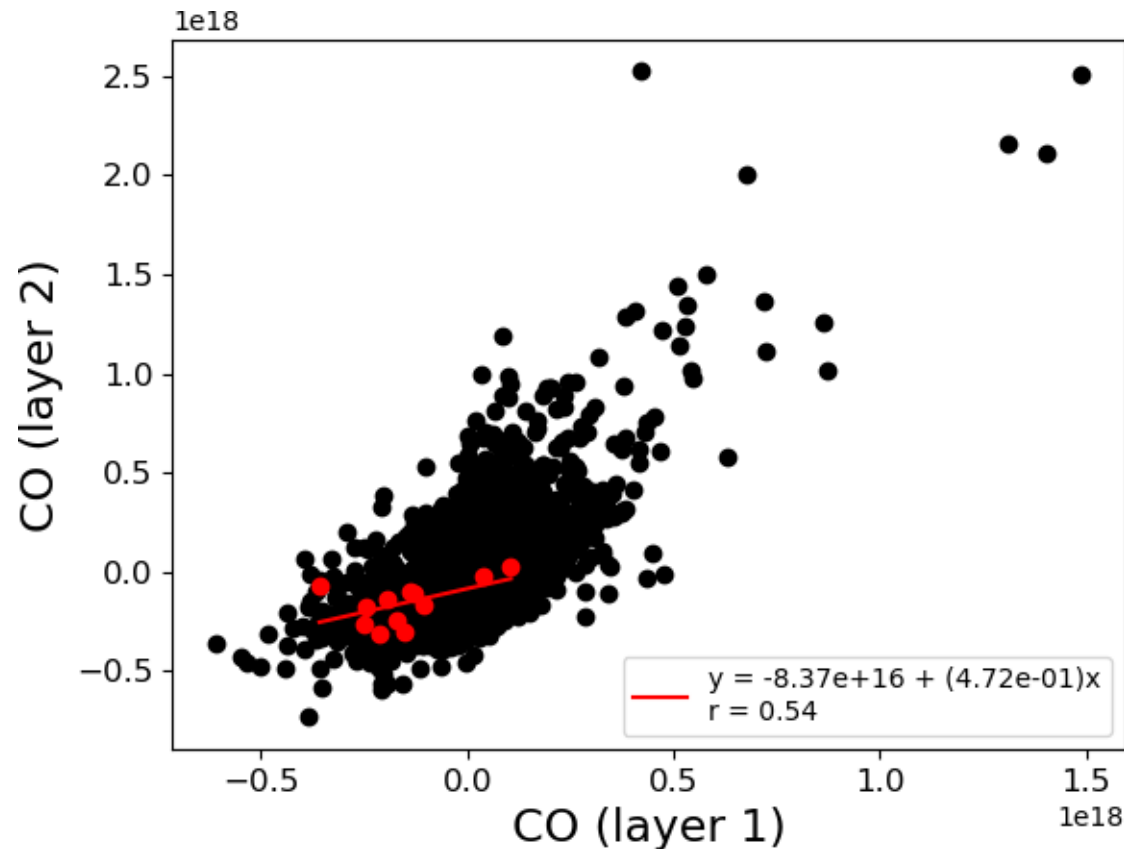
For Toronto, even when partial columns for the regions labeled as 'layer 2' (I2) during folds were plotted (partial columns enclosing levels closer to surface), absolute values of the correlation coefficients were greater than those obtained when all dots were taken into account (scatter plots not show):

$$r_{\text{red dots, I2}} (\text{CH}_4, \text{O}_3) = -0.70 \quad r_{\text{red dots, I2}} (\text{N}_2\text{O}, \text{O}_3) = -0.72$$

$$r_{\text{red dots, I2}} (\text{O}_3, \text{CO}) = -0.65$$

\* I1 -> 5 - 15 km and I2 -> 0.2 - 15 km

Additionally, the pair CO (layer 1) - CO (layer 2) was also plotted:



Only red dots:  $r = 0.54$ , slope = 0.47

All dots:  $r = 0.68$ , slope = 1.21

Based on the slope differences, it is likely that CO in the region labeled as 'I1' (5 - 15 km) contributes less to CO in the region labeled as 'I2' (0.2 - 15 km) during tropopause folds as the Upper Troposphere (UT) receives low-CO air from the stratosphere (see the vertical profiles).

## References

Barrett, B. S., Raga, G. B., Retama, A., and Leonard, C. (2019). A multiscale analysis of the tropospheric and stratospheric mechanisms leading to the March 2016 extreme surface ozone event in Mexico City. *Journal of Geophysical Research: Atmospheres*, **124**. <https://doi.org/10.1029/2018JD029918>

Knowland, K. E., Ott L. E., Duncan, B. N., and Wargan, K. (2017). Stratospheric Intrusion-Influenced Ozone Air Quality Exceedances Investigated in the NASA MERRA-2 Reanalysis. *Geophysical Research Letters*, **44**, 10691-10701. <https://doi.org/10.1002/2017GL074532>

Mohanakumar, K. (2008). *Stratosphere Troposphere Interactions. An Introduction*. Springer.

Sprenger, M., Croci Maspoli, M., and Wernli, H. (2003). Tropopause folds and cross-tropopause exchange: A global investigation based upon ECMWF analyses for the time period March 2000 to February 2001. *Journal of Geophysical Research*, **108**. doi:10.1029/2002JD002587